JOURNAL OF MATERIALS SCIENCE 28 (1993) 3601–3611

AFM, SEM and XPS characterization of PAN-based carbon fibres etched in oxygen plasmas

R. J. SMILEY, W. N. DELGASS
School of Chemical Engineering, Purdue University, West Lafayette, IN 47907, USA

Atomic force microscopy (AFM), scanning electron microscopy (SEM), and X-ray photoelectron spectroscopy (XPS) have been used to investigate changes in topography and surface chemical functionality on PAN-based carbon fibres exposed to low-temperature, low-power, oxygen plasmas. Unsized, type II, Cellion 6000 carbon fibres were treated in oxygen plasmas for 2–60 min at a power of ~25 W. Increasing treatment time caused an increase in oxidation from surface alcohol(ether) to carbonyl and carboxyl species, but the total amount of oxidized carbon near the surface remained constant. SEM confirmed that treatments longer than 15 min resulted in pitting on the fibre surface, but even treatments of 60 min did not significantly reduce the overall fibre diameter. AFM showed surface morphology changes after oxygen plasma treatments for 2 and 15 min. 1 μm × 1 μm AFM scans of untreated fibres showed processing grooves with a distribution of depths. Enlarged images along these grooves revealed that their walls were smooth. Oxygen plasma treatments of 2 min roughened fibre surfaces and created holes of the order of 50 nm evenly distributed with a spacing of 150 nm along the bottoms of the grooves. Treatment for 15 min smoothed the overall topography and resulted in smaller holes, of the order of 5–10 nm, with a spacing of < 50 nm. Calculated RMS roughnesses from the AFM data showed an initial increase in roughness with treatment, followed by a decrease to final values lower than those for untreated fibres.

1. Introduction

Compared to conventional materials such as steel and aluminium alloys, carbon fibre composites have low densities and high strengths and moduli that give them superior strength-to-weight properties. Because the composite interface transfers stresses from the matrix to the fibres, its properties directly affect the shear and delamination resistance of the material. In addition, compression strength, transverse strength, and resistance to attack by the environment are strongly dependent on the interfacial properties. Because bonding at the interface depends on both chemical and mechanical interactions, careful characterization of fibre surface chemistry and morphology is necessary to understand and manipulate interfacial, and ultimately, composite properties.

Much research on carbon fibres has centred on studying chemical functionality changes on surfaces after various treatments. XPS has been a key tool in these studies because of its surface sensitivity and ability to distinguish chemical functional groups [1–6]. Fibre treatments are generally divided into oxidative and non-oxidative methods. Oxidative techniques can be further subdivided into high-temperature gas-phase oxidation [7], plasma treatments [8–12], and liquid-phase oxidation including acid and electrochemical treatments [13–15]. Non-oxidative techniques generally include whisker formation [16], carbon deposition [17], and polymer grafting [18, 19]. Many of these studies have shown that pretreatments before fibre contact with a matrix result in improved interfacial bonding, but little is known about the adhesion mechanisms involved. Additional research is necessary to determine how both physical and chemical interactions between the fibre surface and the matrix affect the stress–strain behaviour of the finished material.

Plasma treatments have been shown in the literature to be an effective way to modify chemical functionality on carbon fibre surfaces [8–12]. By changing plasma gases and process parameters, such as r.f. power, reaction time, and reactor pressure, treatments can focus on improving either structure or chemical activity [20–22]. Compared to plasma-gas treatments, more conventional oxidative treatments such as high-temperature oxygen or strong acid oxidation often introduce dramatic fibre morphology and strength changes [20]. Ismail and Vangsness studied treated pitch-based fibres with SEM and showed that dramatic fibre damage resulted from harsh high-temperature gas oxidation, but little or no damage accompanied low-temperature plasma treatments

0022–2461

[23]. In addition, Xie and Sherwood [8] showed with XPS and X-ray diffraction (XRD) that electrochemical treatments of pitch-based carbon fibres affected fibre bulk and surface structure, while microwave plasma treatments only changed surface structure.

Although plasma treatments can be less destructive than other oxidative methods, many studies using high-power microwave or r.f. energy to generate plasmas have reported significant fibre damage [9, 10, 23–25]. In all cases, prolonged treatments resulted in significant etching and pitting on the fibre surface. For instance, Xie and Sherwood [8, 9] studied the effect of 50 W oxygen- and air-plasma treatments on pitch and PAN-based carbon fibres. XPS results showed that microwave plasmas increased both oxygen and nitrogen surface functionality, but SEM analysis revealed significant reduction of fibre diameters and mass. Even short treatments of 2.5 min in air plasmas were enough to roughen and pit surfaces. Treatments of 30 min or longer were claimed to destroy fibre samples completely [8]. Oxygen plasmas were found to be more reactive than air plasmas, and exposures longer than 10 min significantly reduced fibre mass [9]. Mujin *et al.* [10, 25] also studied fibres treated by high-power low-temperature oxygen plasmas. Mechanical testing and SEM revealed that treatments resulted in lowered tensile strengths and reduced overall fibre diameters.

Only Jones and Sammann [26] have studied the effect of low-power plasmas on fibre surfaces. Ammonia, nitrogen, air and argon plasmas were investigated in an attempt to introduce nitrogen and oxygen functionality on fibre surfaces. They showed qualitatively by angle-resolved XPS (ARXPS) and SEM that 1 W r.f. plasmas were effective at introducing functionality without etching or pitting surfaces. Quantitative ARXPS results showed that chemical change only occurred in the first few atomic layers ~ 1.2–1.5 nm.

Although much work has concentrated on tailoring the fibre-surface functionality to improve chemical attractions at the interface, only a few studies have considered modifying fibre morphology in order to enhance physical adhesion. Interfacial adhesion includes a mechanical interlocking mechanism which is related to surface roughness and fibre porosity. In general, surface roughness will increase physical bonding contributions provided the matrix can wet the fibre surface. Some studies have used BET measurements to follow surface-area changes resulting from various treatments. In particular, Hoffman *et al.* [27] physically adsorbed krypton and chemisorbed oxygen on to treated fibre surfaces to measure total fibre surface area, and the concentration of chemical bonding sites, respectively. Furthermore, Ismail [28] used krypton and nitrogen adsorption to determine effects of plasma treatments on rayon fibre surface area and microporosity. Although these adsorption techniques provide a measure of global surface properties, they do not reveal local properties.

Recently, STM has provided a means of characterizing local fibre surface topography [27, 29–34]. STM has advantages over conventional microscopy techniques, such as SEM [35–37] and TEM [38, 39], because it can non-destructively and quantitatively investigate surfaces in air down to the atomic scale without special sample preparations. Hoffman *et al.* [27, 29, 30] have shown the potential of STM for monitoring small topography changes on both pitch and PAN-based carbon fibres resulting from various treatments. STM, however, requires a conducting sample. Consequently, any adsorbate or coating on the fibre surface which interrupts the conducting nature of the sample will cause the tunnelling tip to crash into the surface. More recently, AFM has been used to image both non-conducting as well as conducting surfaces [40, 41]. The technique combines both stylus profilometry and tunnelling microscopy methods. Instead of monitoring changes in tunnelling current, AFM profiles a surface by utilizing the interatomic forces between a sharp tip on a cantilever and the sample surface. AFM has been used to image graphite and other carbon materials [42], but until now has not been used to investigate carbon fibres [50].

In the present work we investigated qualitatively and quantitatively the effect of low-power low-temperature r.f. oxygen-plasma treatments on PAN-based carbon fibres. By lowering plasma-power levels to 25 W, we were able to treat fibres in an oxygen environment for 60 min. Treatments introduce oxygen functionality on the outermost surface without seriously changing the overall fibre diameter. Hence, fibre mechanical properties should remain unchanged. Chemical functionality changes were monitored by XPS, while surface morphology changes were followed at the micrometre scale by SEM and down to the 5 nm scale by AFM.

2. Experimental procedure

The PAN-based carbon fibre samples used in this work are unsized type II Cellion 6000 fibres obtained from the Celanese Corporation. These fibres are classified as high-tensile (3.62 GPa), intermediate modulus (234 GPa) materials [43]. Plasma treatments were performed in a Harrick PDC-3XG r.f. plasma chamber using about 25 W power at pressures of 10^{-2} torr (1 torr = 133.322 Pa). Fibre temperatures are assumed to have remained around room temperature. No temperatures were measured *in situ*, but the samples were always cool immediately after treatment. Fibres, placed parallel to and touching each other, were arranged in multiple layers on an XPS sample holder and held down by a gold cover ring. The entire holder was placed inside the glass plasma chamber which was evacuated and purged with oxygen several times before the r.f. power was turned on. Fibres were treated in the oxygen plasma for 2–60 min.

After treatment, samples were immediately transferred through the air to a Perkin–Elmer 5300 XPS. Spectra were collected at a base pressure of about 10^{-9} torr using a magnesium ($K_{\alpha 1,2} = 1253.6$ eV) X-ray source operated at 15 kV and 300 W. The total spectrometer broadening was of the same order as the X-ray linewidth, about 0.7 eV for magnesium, at the electron pass energy of 8.95 eV. The spectrometer was

calibrated by setting the binding energies of the Au $4f_{7/2}$ and Cu $2p_{3/2}$ level values to 84.0 and 932.7 eV, respectively.

XPS spectra were computer fit in order to determine the chemical state and quantity of specific species on fibre surfaces. Curve fitting was carried out using a non-linear least squares fitting program with a Gaussian/ Lorentzian sum function. The only parameter constrained in the fitting routine was the Gaussian/ Lorentzian mix (fraction Gaussian) for the oxidized carbon species which was set to 0.5. Intensities, peak positions, linewidths, and exponential tail height and slope for the main carbon peak were all optimized by the fitting routine. The main peak was fit with an exponential tail to account for its asymmetric character, which arises because the carbon species is conducting and exhibits the same core–hole coupling observable in most metals [44, 45].

Scanning electron micrographs were obtained on a Jeol JSM-840 microscope with a beam voltage of 10 keV, working distances between 10 and 18 mm, and probe current of 6×10^{-11} A. Untreated and treated carbon fibres were aligned side by side and mounted on an aluminium sample stud by copper conducting tape. The sample stud was then sputter coated with a 200 nm Au/Pd layer in order to reduce charging on fibre surfaces. Images were recorded on Polaroid type 55 positive–negative film. Fibre diameters were measured directly from these images.

AFM images were collected on a Park Scientific Instruments (PSI) SFM-BD2 microscope in the contact mode, at a constant interatomic repulsive force between the tip and surface. The cantilevers were also obtained from PSI and were micro-fabricated from low-stress Si_3N_4. The V-shaped microlever is 200 μm long, 36 μm wide, and has a theoretical force constant and resonant frequency of 0.064 Nm^{-1} and 17 kHz, respectively. The integrated pyramidal tip has a nominal radius of less than 40 nm. All images were collected with a constant force between 5 and 15 nN and a line-scan frequency between 0.5 and 1 Hz.

Root-mean-square roughnesses (RMS), average roughnesses, and maximum peak-to-valley (PTV) distances were determined from AFM data using PSI data analysis software.

3. Results and discussion

3.1. Surface composition

Fig. 1a–f show the curve-fit C(1s) XPS spectra for untreated Cellion 6000 fibres as well as fibres treated in oxygen plasma for 2, 5, 15, 30 and 60 min. Table I summarizes the peak positions, area percentages, linewidths, and the percentages of the spectral area corresponding to the sum of all the oxidized carbon states for the spectra in Fig 1. Table I also gives the Gaussian/ Lorentzian mix and asymmetric tail height and slope for the main graphitic peaks.

All carbon fibre C(1s) spectra exhibit a large peak centred at 284.4 eV with an extensive shoulder at higher binding energies. The sum of the symmetrical peak at 284.4 eV and the asymmetrical peak at 285 eV in Fig. 1a represents the total area of the main carbon

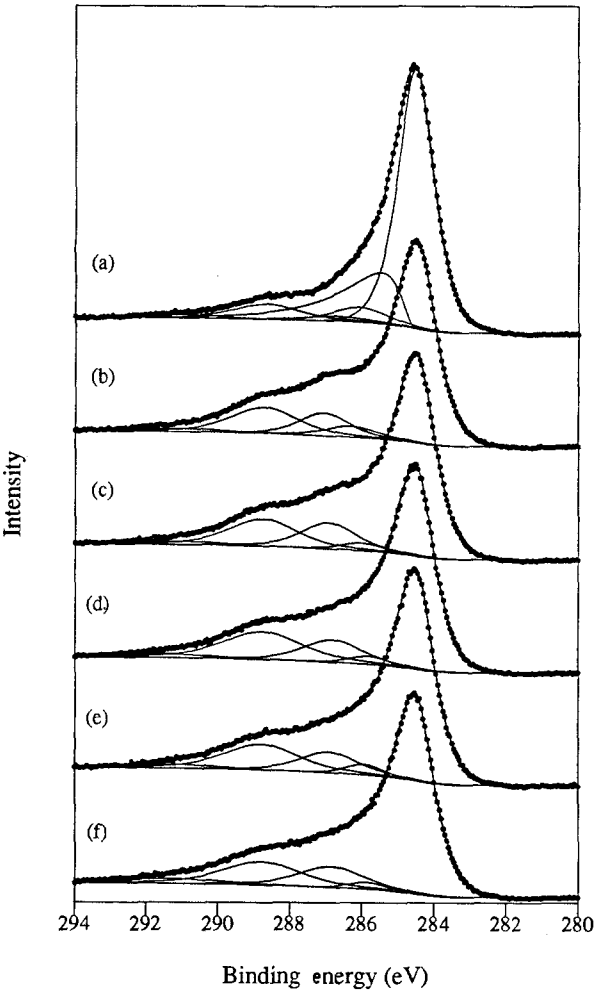

Figure 1 XPS C(1s) spectra of Cellion 6000 carbon fibres treated for various times in an oxygen plasma. (a) Untreated, (b) 2 min, (c) 5 min, (d) 15 min, (e) 30 min, (f) 60 min.

peak. In order to simplify the figure, the area contribution from the graphitic peak was left off spectra 1b–f. All samples have linewidths of 1.2 eV for the main carbon peak, which indicates that the overall graphitic character remains unchanged with treatment. A correlation between graphite order and XPS main peak width has been reported in the literature [46]. To confirm this relation on our instrument, we analysed an HOPG sample before and after argon bombardment for 5 and 10 min and found a corresponding increase in the main peak linewidth from 0.7 eV to 1.1 eV and then to 1.3 eV. The shoulder at higher binding energies in Fig. 1 is resolved into four peaks shifted from the main peak by approximately 1.5, 2.3, 4.2, and 6.5 eV and corresponding, respectively, to alcohol and/or ether, carbonyl, and carboxyl chemical states as well as a characteristic plasmon loss.

Initial estimates for these peak positions were calculated from the relative binding energy shifts for small gas-phase molecules with similar functional groups. Siegbahn *et al.* [47] calculated C(1s) electron binding energy shifts of 1.6, 3.1, and 4.7 eV, respectively, for ethanol, acetone, and acetic acid using the complete neglect of differential overlap (CNDO) molecular orbital method. Even though these calculations are for small molecules in free space, the increasing trend in chemical shift as a function of increasing carbon charge would be expected to also hold for surface

TABLE I Fitted parameters for C(1s) spectra in Fig. 1

Treatment	Treatment time (min)					
	0	2	5	15	30	60
Graphite						
BE (eV)	284.5	284.5	284.5	284.5	284.5	284.5
Area (%)	81.9	70.8	69.8	67.7	70.9	69.5
FWHM (eV)	1.2	1.2	1.2	1.2	1.2	1.2
Tail slope	0.299	0.368	0.358	0.343	0.341	0.368
Tail height	0.498	0.499	0.507	0.499	0.497	0.487
G/L mix (fraction Gaussian)	0.30	0.29	0.32	0.32	0.30	0.30
Oxide 1						
BE (eV)	286.0	286.3	286.0	285.8	285.9	285.8
Area (%)	5.9	4.5	2.5	2.3	2.9	2.0
FWHM (eV)	1.7	1.7	1.4	1.3	1.2	1.2
Oxide 2						
BE (eV)	286.7	287.0	286.9	286.8	286.9	286.8
Area (%)	2.4	8.9	11.1	10.3	9.2	10.5
FWHM (eV)	2.2	1.7	1.8	1.9	1.9	2.1
Oxide 3						
BE (eV)	288.6	288.7	288.7	288.7	288.8	288.8
Area (%)	7.7	13.5	14.3	16.9	14.7	14.1
FWHM (eV)	2.2	2.2	2.2	2.6	2.5	2.6
Plasmon						
BE (eV)	291.0	291.0	291.1	291.4	291.0	291.2
Area (%)	2.1	2.4	2.3	2.8	2.3	3.8
FWHM (eV)	2.4	2.8	2.5	2.8	2.3	3.2
Total oxide						
Area (%)	16	27	28	30	27	27

carbon oxidation states. The peak position estimates along with that for the plasmon peak were entered into the curve-fitting routine and optimized by non-linear least squares analysis. As shown in Table I, even for a variety of sample pretreatments, fitted parameters such as peak positions for the various oxidized carbon species; tail slope, height, and position for the main carbon peak; and all linewidths were reproducible without any constraints except for a fixed Gaussian/Lorentzian mix for the oxidized carbon peaks. Thus, the binding energy shift assignments to various carbon oxidation states held to narrow tolerances over a variety of surface conditions and were consistent with both initial estimates and values reported in the literature for carbon fibres [10, 25, 46].

Fig. 2a–f show the corresponding curve-fit O(1s) spectra, while Table II gives the fitted parameters. Also tabulated are the ratio of total oxygen to total carbon intensities, corrected by their respective Scofield cross-sections [48].

XPS O(1s) raw data consist of a large, featureless envelope of peaks which range in binding energy from 530–535 eV. There is some variation in the literature concerning the best method of fitting the O(1s) region. Desimoni *et al.* [49] fit their O(1s) data with three peaks at 531, 532.5 and 534 eV, which they assign, respectively, to carbonyl groups, alcohol groups, and either carboxyl groups or adsorbed water. Xie and Sherwood [1, 8, 9] use two or three peaks at 531–532, 533 and 535.5 eV which they assign in a similar way to Desimoni *et al.* In this study only two peaks, at 531.5 and 533.0 eV, are necessary to give a good fit. For this investigation, we concern ourselves primarily with the

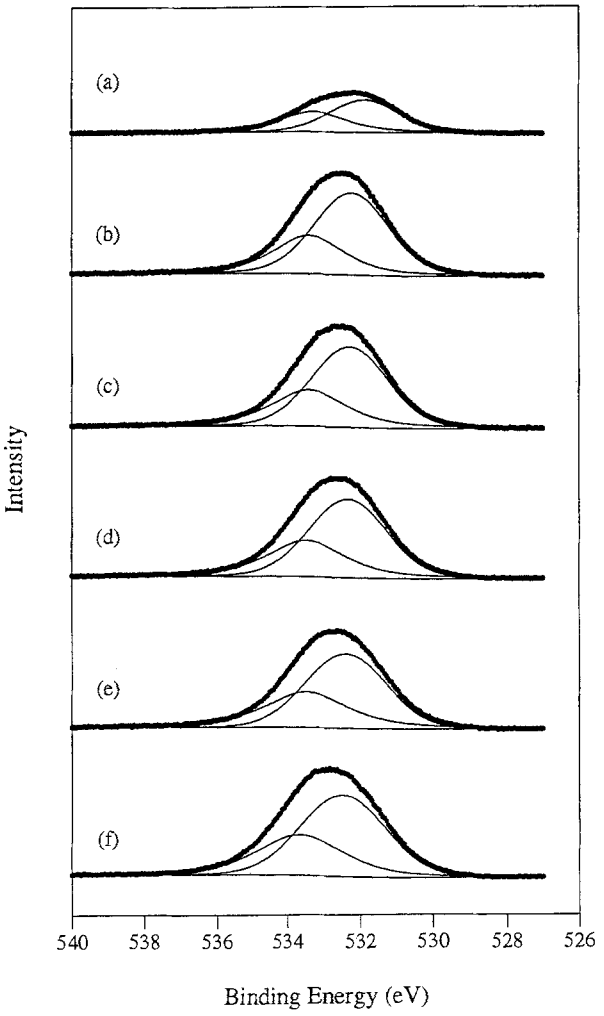

Figure 2 XPS O(1s) spectra of Cellion 6000 carbon fibres treated for various times in an oxygen plasma. (a–f) as Fig. 1.

TABLE II Fitted parameters for O(1s) spectra in Fig. 2

	Treatment time (min)					
	0	2	5	15	30	60
Peak 1						
BE (eV)	531.9	532.2	532.2	532.3	532.4	532.4
Area (%)	56.2	64.9	63.8	62.8	60.0	62.1
FWHM (eV)	2.2	2.4	2.5	2.5	2.6	2.7
G/L mix (fraction Gaussian)	0.93	0.84	0.89	0.89	0.97	0.91
Peak 2						
BE (eV)	533.3	533.4	533.4	533.5	533.5	533.6
Area (%)	43.8	35.1	36.2	37.2	40.0	37.9
FWHM (eV)	2.1	2.3	2.4	2.5	2.7	2.8
G/L mix (fraction Gaussian)	0.28	0.37	0.28	0.27	0.23	0.47
$n(O1s)/n(C1s)$ (%)	16	32	32	33	34	38

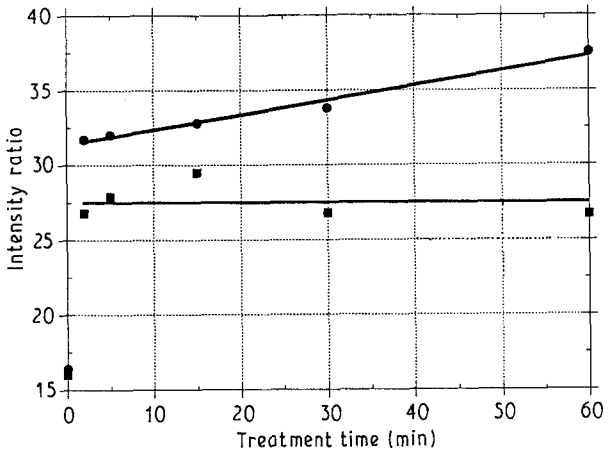

Figure 3 Ratio of cross-section-normalized (●) O(1s)/C(1s) and (■) oxidized-C(1s)/total-C(1s) XPS intensities as a function of oxygen-plasma treatment time.

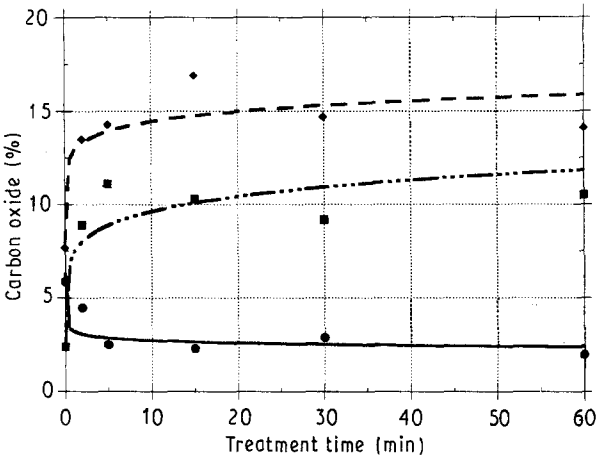

Figure 4 Intensity ratios for (——) alcohol(ether), (— · · —) carbonyl, and (— — —) carboxyl species as a function of oxygen plasma treatment time.

overall O(1s) area and have not tried to assign the chemical state of O(1s) components.

The ratios of different XPS intensities are plotted as a function of oxygen-plasma treatment time in Fig. 3. The $I(O_{1s})/I(C_{1s})$ intensity ratios, normalized by cross-sections, increase linearly from 32% to 38% for fibres treated for 2–60 min. The total C(1s) oxide area percentages, given in Table I, are calculated by summing the total oxidized carbon area and dividing by the overall carbon area. These ratios remain fairly constant at about 27.5% with increasing treatment times. The individual alcohol(ether), carbonyl, and carboxyl carbon area percentages are plotted as a function of treatment time in Fig. 4. Although the absolute peak areas include a considerable uncertainty in peak linewidths, the area percentages in Fig. 4 show the simple trend that as alcohol(ether) intensity decreases, both carbonyl and carboxyl intensities increase. In addition, Figs 3 and 4 both confirm that oxygen plasmas introduce most of the surface functionality during the first 2 min treatment.

N(1s) and Si(2p) XPS spectra, not shown, were also collected along with the O(1s) and C(1s) regions. They show that untreated Cellion 6000 carbon fibres contain 3% nitrogen and trace amounts of silicon. Oxygen-plasma treatments cause some change in the amount of nitrogen present on the surface, but it never exceeds 5%. Longer plasma treatments show an increase in silicon, in the oxidized SiO_2 state, on the surface. XPS analysis of Si(2p) regions showed that intensities levelled off after treatments of 5 min and remained less than 2% of the total carbon intensity, normalized for cross-section. Total oxidized carbon percentages and main graphitic linewidths remain fairly constant throughout treatment and give evidence that plasma treatments are mild enough to attack a finite number of active carbon sites initially present on the fibre surface but are unable to create new reactive sites.

3.2. Surface morphology

Fig. 5a and b show typical SEM cross-sectional micrographs at × 12000 for untreated and 60 min treated Cellion 6000 carbon fibres. These fibres have circular cross-sections with average diameters between 6.7 and 6.9 μm. Fig. 5b shows that long treatments maintain the circular cross-section and leave

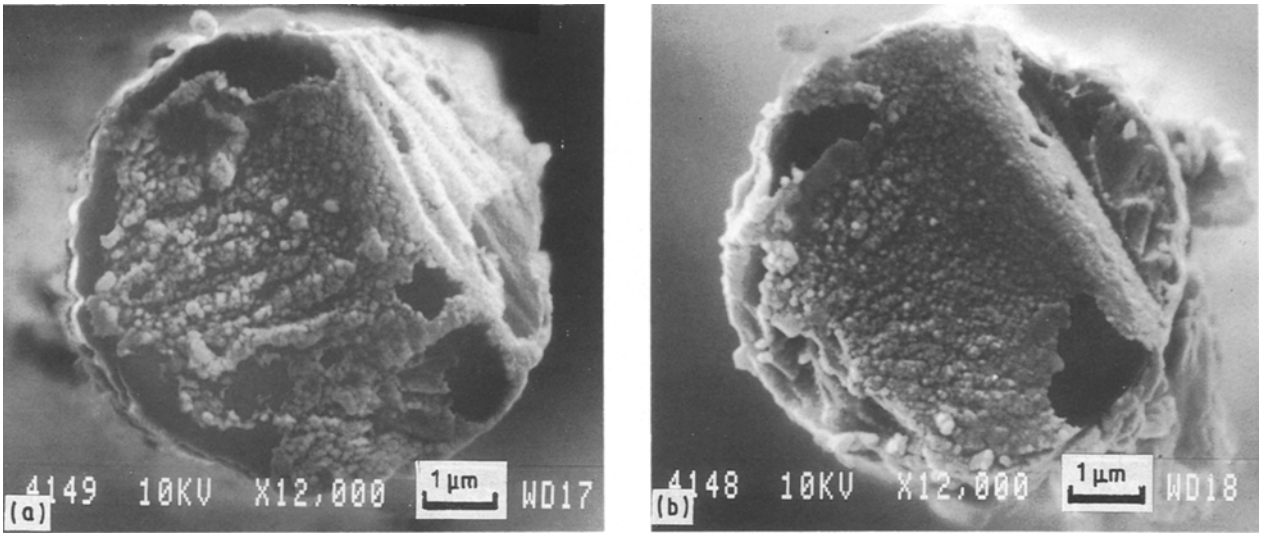

Figure 5 Transverse scanning electron micrographs (12,000X) of (a) untreated and (b) 60 min treated Cellion 6000 carbon fibres.

some large boulder-like features on the surface. Fig. 6a–f are longitudinal micrographs at × 12000 for untreated and 2, 5, 15, 30 and 60 min oxygen-plasma treated fibres, respectively. Side views of untreated fibres reveal relatively smooth surfaces with axial striations left by fibre manufacturing, as in Fig. 6a. The axial grooves present on images of untreated fibres remain unchanged after plasma treatments of 15 min or less, Fig. 6b–d. Treatment times longer than 15 min result in an overall smoothing of the surface, qualitatively seen by the greater breadth and shallowness of the grooves. In addition, longer treatment times of 30 and 60 min result in the appearance of bumps and pits on the fibre surfaces, Fig. 6e and f. Figs 5 and 6 confirm that our oxygen-plasma treatments did not attack the interior of the fibre or significantly change the overall fibre diameter.

Formation of surface pits has been described in the literature for carbon fibres treated by r.f. and microwave plasmas [1, 23]. Xie and Sherwood [9] have shown that microwave air-plasma treatments of 2.5 min initially roughen the fibre surface. Longer treatments did not continue to create new holes, but ultimately resulted in an overall smoothing on the SEM length scale. In addition, Xie and Sherwood reported that treatments of 2.5, 5, 10 and 20 min caused weight losses of 2.61%, 5.97%, 12.06% and 23.17%, respectively. Measurements directly from the published micrographs show that the diameter of the fibre treated in an air plasma for 20 min was reduced by about 14% compared to the untreated one. The pitting of fibre surfaces most likely results from plasma gases strongly attacking defect-rich or edge-carbon sites, but further research is necessary to understand the final smoothing mechanism. Clearly, low-power treatments delay surface pitting and slow overall etching of fibres.

In order to investigate local structure on a smaller scale than is accessible by SEM, AFM images were collected for untreated fibres and those treated in an oxygen plasma for 2 and 15 min. Fig. 7a is a 1 µm × 1 µm tilted perspective view AFM image of untreated Cellion 6000 with a grey scale ranging from 0–25 nm. Fig. 7b shows the corresponding top-view perspective of the same image. The grooves present in the figures are the same as those readily seen by SEM. As illustrated in Fig. 7a and b, these axial grooves are unevenly spaced from 40–120 nm apart and have a distribution of depths ranging from 1–7 nm.

1 µm × 1 µm area (a) tilted and (b) top-view images of fibres treated in an oxygen plasma for 2 and 15 min, are shown in Figs 8 and 9, respectively. The grey scales are different for the two images and range from 0–50 nm for 2 min treatment and 0–10 nm for 15 min treatment. From a comparison of the grey scales for Figs 7–9, it appears that the fibre surfaces go through an initial roughening after short plasma treatment, followed by an overall smoothing as treatment time is increased. RMS roughness, average roughness, and maximum PTV values calculated from AFM images in Figs 7–9 are given in Table III and quantitatively support this observation.

Fig. 10a–c show enlarged images along the grooves labelled A, B and C in Figs 7–9. These increased magnifications are necessary to accentuate the fine structure resulting from surface treatment. Fig. 10a is a 150 nm × 600 nm zoom along a groove on an untreated fibre. The grey scale ranges from 0–5 nm. This enlarged image shows that the groove walls are relatively straight and smooth. Compared to the untreated fibre, the 2 min treated sample, Fig. 10b, shows dramatically different surface features. The grooves are no longer straight and smooth but contain holes with diameters of the order of 50 nm, which are distributed at 150 nm intervals. The holes are circular in shape and are approximately 10–20 nm deep along this groove. Although they are not shown, enlargements along other grooves in the sample corresponding to Fig. 8 show that the holes can be shallower, approximately 5–8 nm, but always maintain the 50 nm size and regular spacing of 150 nm. Fibres treated for 15 min in oxygen plasma show still different surface morphology, Fig. 10c. Overall roughness is reduced to values lower than for the untreated fibres,

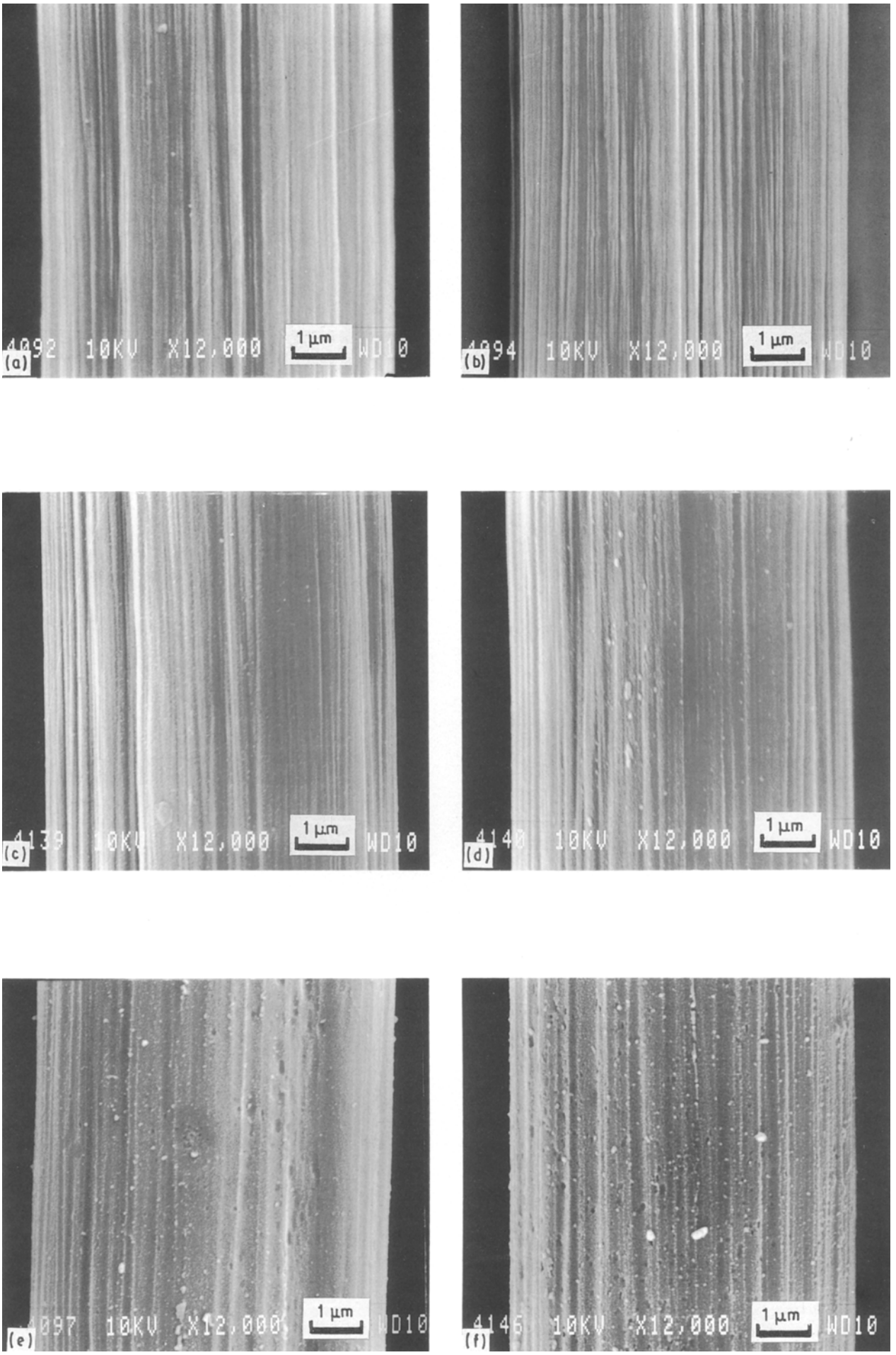

Figure 6 Longitudinal scanning electron micrographs (12 000X) of (a) untreated, (b) 2 min, (c) 5 min, (d) 15 min, (e) 30 min, and (f) 60 min treated Cellion 6000 carbon fibres.

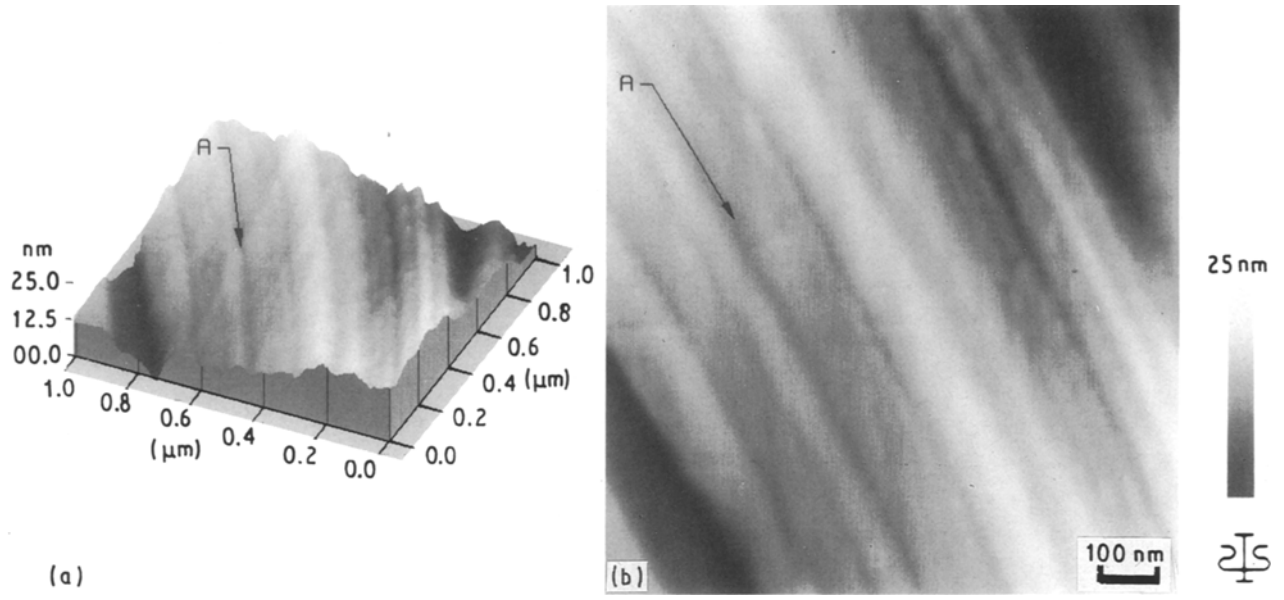

Figure 7 AFM image of untreated Cellion 6000 carbon fibre; (a) tilted view and (b) top view.

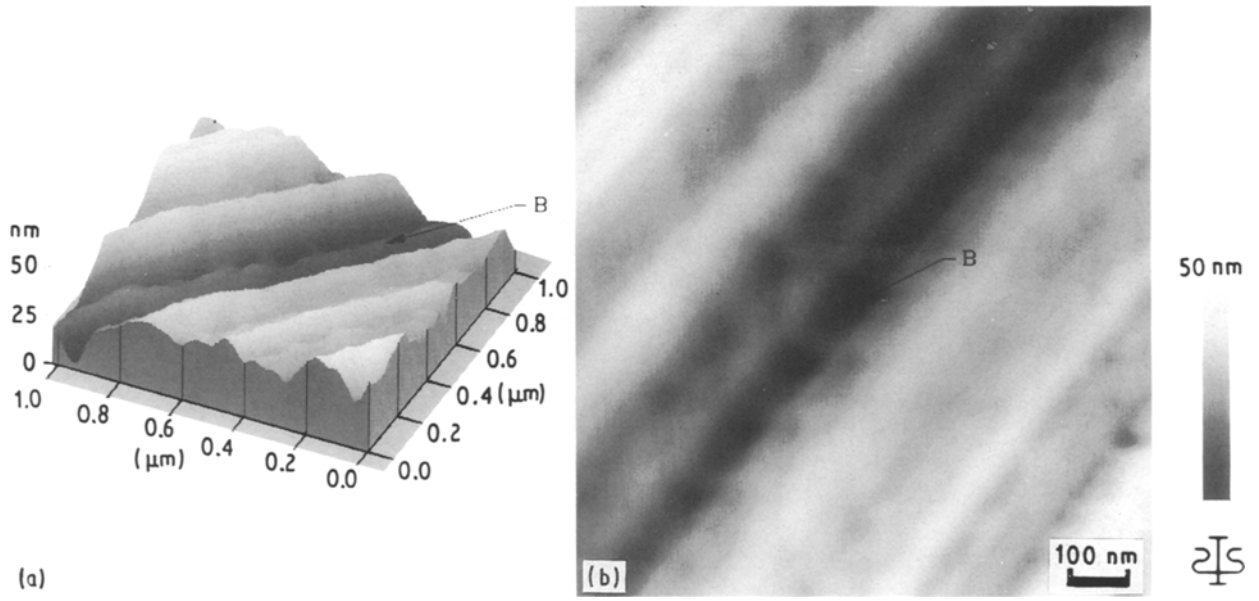

Figure 8 AFM image of a Cellion 6000 carbon fibre treated in an oxygen plasma for 2 min; (a) tilted view and (b) top view.

as shown by the grey scale ranging from 0–1.5 nm. Fig. 10c shows circular holes similar to those found on 2 min treated surfaces, but the diameters and interval spacings are smaller, of the order of 5–10 and < 50 nm, respectively.

Long oxygen-plasma treatment tends to smooth the overall surface by widening grooves faster than it etches into the bottoms of the grooves. The appearance of the holes in the bottoms of the grooves at early stages of treatment, however, suggests that the outer surface carbon layers are heterogeneous. The regular spacings of these holes must be related to the structure and corresponding reactivity of the fibre surface. Many studies have used TEM to characterize fibre bulk and surface structure. TEM has shown carbon fibres are made up of basic structural units (BSU) with characteristic shape and size described by intraplanar distance, L_a, interplanar distance, L_c, and radius of curvature, r_t [38, 39]. Guigon and co-workers [38, 39] model fibre surfaces as large wrinkled sheets where the

TABLE III AFM roughness for untreated and oxygen-plasma treated fibres

Treatment time (min)	RMS (nm)	AVG (nm)	PTV (nm)
0	3.8	3.0	22.2
2	9.0	7.3	50.9
15	2.0	1.8	8.3

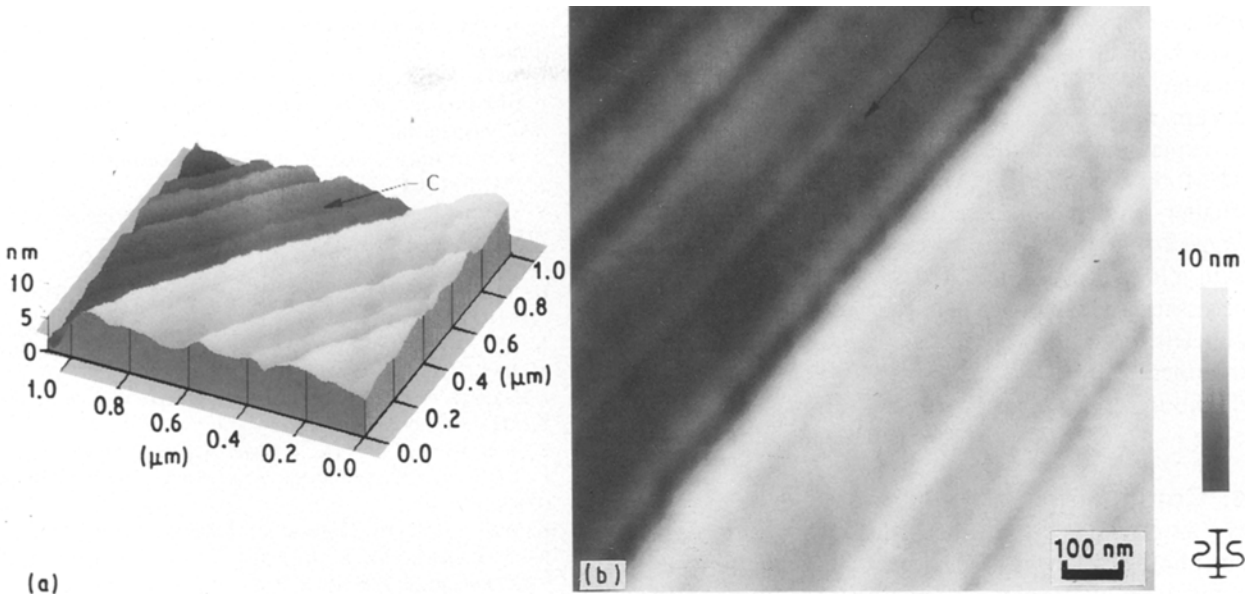

Figure 9 AFM image of a Cellion 6000 carbon fibre treated in an oxygen plasma for 15 min; (a) tilted view and (b) top view.

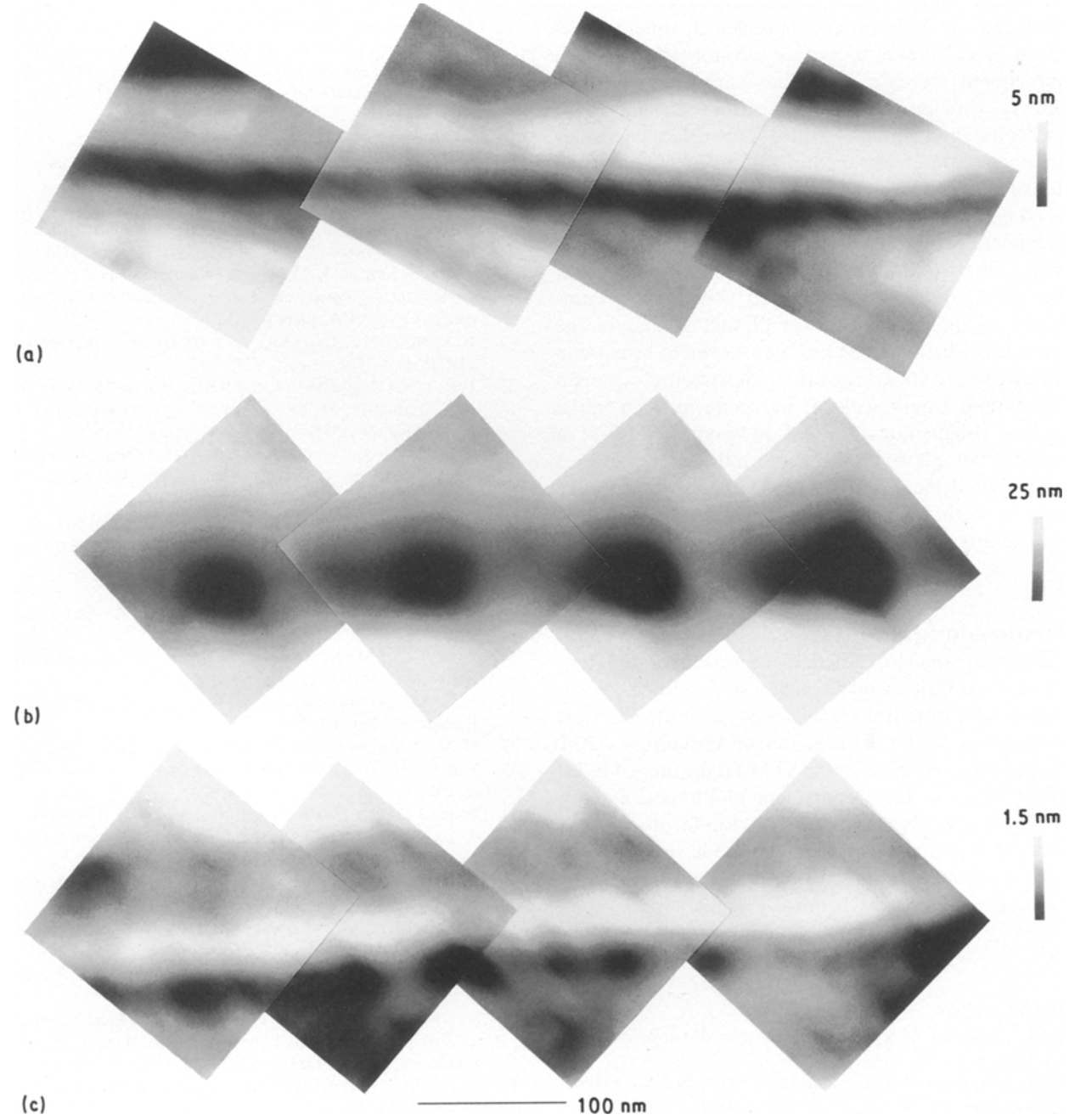

Figure 10 Enlarged AFM images along grooves for (a) untreated, (b) 2 min treated, and (c) 15 min treated Cellion 6000 carbon fibres.

BSUs are associated in a zigzag form with tilt and twist boundaries. PAN-based, high-tensile carbon fibres have typical L_a and L_c values of around 1.6 and 2.5 nm, respectively. These parameters seem too small to explain the heterogeneous reactivity revealed by AFM. STM studies by Marshall and Price [34] on smaller diameter fibres after more severe oxidation suggest that the surface contains graphitic platelets with a long dimension of 100 nm. Further research is necessary to explore possible relationships of such platelets, initial fibre processing conditions, and pretreatment procedures to the surface heterogeneity of the fibres.

4. Conclusions

We have followed both the surface composition and morphology changes of Cellion 6000 carbon fibres as a function of oxygen plasma treatment time. XPS results show that oxidized carbon species including alcohols(ethers), carbonyls, and carboxyls can be introduced on fibre surfaces. Longer treatment times result in a decrease in surface alcohols(ethers) and a subsequent increase in surface carbonyls and carboxyls. Low-power low-temperature plasma treatments are mild enough to introduce surface chemistry changes without the creation of many new carbon active sites. SEM demonstrated that even treatments of 60 min did not significantly change the overall fibre diameter. Scanning electron micrographs of treatments longer than 15 min did show pitted surfaces, but the pitting process was delayed considerably compared to similar high-power plasma studies in the literature. Finally, AFM has been shown to be a useful technique for studying surface morphology changes on a small length scale. It has confirmed an initial surface roughening followed by a smoothing as a function of plasma treatment and has revealed a heterogeneity in reactivity along the bottoms of the grooves with a length scale of about 150 nm in the roughening stage.

Acknowledgements

The authors thank Celanese Corporation for donating the unsized Cellion 6000 carbon fibres. SEM micrographs were obtained on microscopes in the Electron Microscopy Center in the School of Agriculture. AFM images were obtained in the STM laboratory of R. G. Reifenberger in the Department of Physics, and we thank him, M. Paniccia, and T. S. Lin for discussions of AFM experiments and results. We have also benefitted from many stimulating discussions with J. M. Caruthers, School of Chemical Engineering.

References

1. Y. XIE and P. M. A. SHERWOOD, *Appl. Spectrosc.* **44** (1990) 1621.
2. G. E. HAMMER and L. T. DRZAL, *Appl. Surf. Sci.* **4** (1980) 340.
3. G. K. A. KODOKIAN and A. J. KINLOCH, *J. Mater. Sci. Lett.* **7** (1988) 625.
4. Y. NAKAYAMA, F. SOEDA and A. ISHITANI, *Carbon* **28** (1990) 21.
5. K. WALTERSSON, *Fibre Sci. Technol.* **17** (1982) 289.
6. P. DENISON, F. R. JONES and J. F. WATTS, *Surf. Interface Anal.* **9** (1986) 431.
7. S. R. KELEMEN and H. FREUND, *Energy Fuels ACS J.* **2** (1987) 111.
8. Y. XIE and P. M. A. SHERWOOD, *Appl. Spectrosc.* **44** (1990) 797.
9. *Idem, ibid.* **43** (1989) 1153.
10. D. YOUXIAN, W. DIANXUN, S. MUJIN, C. CHUANZHENG and Y. JIN, *Compos. Sci. Technol.* **30** (1987) 119.
11. J. B. DONNET, T. L. DHAMI, S. DONG and M. BRENDLE, *J. Phys. D Appl. Phys.* **20** (1987) 269.
12. I. H. LOH, R. E. COHEN and R. F. BADDOUR, *J. Mater. Sci.* **22** (1987) 2937.
13. T. H. KO and C. H. LIN, *J. Mater. Sci. Lett.* **7** (1988) 628.
14. C. KOZLOWSKI and P. M. A. SHERWOOD, *Carbon* **24** (1986), 357.
15. K. WALTERSSON, *Compos. Sci. Technol.* **23** (1985) 303.
16. R. T. BAKER, M. A. BARBER, P. S. HARRIS, F. S. FEATES and R. J. WAITE, *J. Catal.* **26** (1972) 51.
17. G. DAGLI and N. SUNG, *Polym. Compos.* **10** (1989) 109.
18. V. KRISHNAMURTHY and I. KAMEL, in "Proceedings of the 33rd International SAMPE Symposium", 7–10 March 1988, Anaheim, CA, edited by G. Carrillo, E. D. Newell, W. D. Brown and P. Phelan (Society for the Advancement of Material and Process Engineering, Covina, CA, 1988) p. 560.
19. V. KRISHNAMURTHY and I. KAMEL, *J. Mater. Sci.* **24** (1989) 3345.
20. S. MUJIN, H. BAORONG, W. YISHENG, T. YING, H. WEIQUI and D. YOUXIAN, *Compos. Sci. Technol.* **34** (1989) 353.
21. S. L. KAPLAN, P. W. ROSE, H. X. NGUYEN and H. W. CHANG, in "Proceedings of the 33rd International SAMPE Symposium", 7–10 March, 1988, Anaheim, CA, edited by G. Carrillo, E. D. Newell, W. D. Brown and P. Phelan (Society for the Advancement of Material and Process Engineering, Covina, CA, 1988) p. 551.
22. H. X. NGUYEN, G. RIAHI, G. WOOD and A. POURSARTIP, *ibid.*, p. 1721.
23. I. K. ISMAIL and M. VANGSNESS, *Carbon* **26** (1988) 749.
24. J. B. DONNET, M. BRENDLE, T. L. DHAMI and O. P. BAHL, *ibid.* **24** (1986) 757.
25. S. MUJIN, H. BAORONG, W. YISHENG, T. YING, H. WEIQIU and D. YOUXIAN, *Compos. Sci. Technol.* **34** (1989) 353.
26. C. JONES and E. SAMMANN, *Carbon* **28** (1990) 509.
27. W. P. HOFFMAN, W. C. HURLEY, T. W. OWENS and H. T. PHAN, *J. Mater. Sci.* **26** (1991) 4545.
28. I. M. K. ISMAIL, *Carbon* **28** (1990) 401.
29. W. P. HOFFMAN, V. B. ELINGS and J. A. GURLEY, *ibid.* **26** (1988) 754.
30. W. P. HOFFMAN, W. C. HURLEY, P. M. LIU and T. W. OWENS, *J. Mater. Res.* **6** (1991) 1685.
31. S. N. MAGONOV, H. J. CANTOW and J. B. DONNET, *Polym. Bull.* **23** (1990) 563.
32. N. M. D. BROWN and H. YOU, *Surf. Sci.* **237** (1990) 273.
33. J. P. RABE, M. SANO, D. BATCHELDER and A. A. KALATCHEV, *J. Microsc.* **152** (1988) 573.
34. P. MARSHALL and J. PRICE, *Composites* **22** (1991) 388.
35. A. RAZVAN, C. E. BAKIS and K. L. REIFSNIDER, *Mater. Charact.* **24** (1990) 179.
36. D. L. VEZIE and W. W. ADAMS, *J. Mater. Sci. Lett.* **9** (1990) 883.
37. J. D. MILLER, H. ISHIDA and F. J. J. MAURER, *J. Mater. Sci.* **24** (1989) 2555.
38. M. GUIGON, A. OBERLIN and G. DESARMOT, *Fibre Sci. Technol.* **20** (1984) 177.
39. A. OBERLIN and M. GUIGON, in "Fibre Reinforcements for Composite Materials", edited by A. R. Bunsell (Elsevier Science, New York, 1988) p. 149.
40. G. BINNIG, C. F. QUATE and C. GERBER, *Phys. Rev. Lett.* **56** (1986) 930.
41. T. R. ALBRECHT and C. F. QUATE, *J. Appl. Phys.* **62** (1987) 2599.

42. O. MARTI, B. DRAKE, S. GOULD and P. K. HANSMA, *J. Vac. Sci. Technol. A* **6** (1988) 287.
43. J. B. DONNET and R. C. BANSAL, "Carbon Fibers" (Marcel Dekker, New York, 1990) p. 4.
44. T. TAKAHAGI and A. ISHITANI, *Carbon* **22** (1984) 43.
45. W. N. DELGASS, G. L. HALLER, R. KELLERMAN and J. H. LUNSFORD, "Spectroscopy in Heterogeneous Catalysis" (Academic Press, New York, 1979) p. 286.
46. Y. XIE and P. M. A. SHERWOOD, *Chem. Mater.* **2** (1990) 295.
47. K. SIEGBAHN, C. NORDLING, G. JOHANSSON, J. HEDMAN, P. F. HEDMAN, K. HAMRIN, U. GELIUS, T. BERGMARK, L. O. WERME, R. MANNE and Y. BAER, "ESCA applied to free molecules" (North-Holland, New York, 1971) p. 117.
48. J. H. SCOFIELD, *J. Electron Spectros. Relat. Phenom.* **8** (1976) 129.
49. E. DESIMONI, G. I. CASELLA, A. MORONE and A. M. SALVI, *Surf. Interface Anal.* **15** (1990) 627.
50. W. P. HOFFMAN, *Carbon* **30** (1992) 315.

Received 29 June
and accepted 20 November 1992